



Morphological aspects and optical properties of $\text{Ag}_4\text{P}_2\text{O}_7$

Wyllamanney da S. Pereira^a, Cipriano B. Gozzo^a, Elson Longo^a, Edson R. Leite^b,
Júlio C. Sczancoski^{a,*}

^a Universidade Federal de São Carlos, Department of Chemistry, São Carlos, SP, Brazil

^b Brazilian Nanotechnology National Laboratory, CNPEM, Campinas, SP, Brazil



ARTICLE INFO

Article history:

Received 10 March 2019
Received in revised form 6 April 2019
Accepted 9 April 2019
Available online 9 April 2019

Keywords:

Crystal growth
Luminescence
Spectroscopy
Recrystallization

ABSTRACT

The structural, morphological and optical properties of silver pyrophosphate ($\text{Ag}_4\text{P}_2\text{O}_7$) powders were investigated in detail. This material was synthesized by chemical precipitation (CP), conventional hydrothermal and microwave-assisted hydrothermal. The crystallization of hexagonal $\text{Ag}_4\text{P}_2\text{O}_7$ phase presented a dependence with both temperature and synthesis approach. A system composed of doughnut/hexagonal-shaped microparticles was evidenced for the powders obtained by CP. The hydrothermal treatments modified these particle shapes. Ultraviolet–visible spectra revealed a band gap controlled by indirect electronic transitions. Broadband photoluminescence spectra with maximum emissions in blue region were detected, suggesting the participation of several intermediary energy levels in the band gap.

© 2019 Elsevier B.V. All rights reserved.

1. Introduction

In Physics, color is defined as a visual sensation received by the brain, as a result from the detection of light interacted (absorbed, reflected and/or transmitted) with an object [1]. The human eyes have capacity of perceiving a small part of the spectrum of electromagnetic waves, i.e., an interval from 380 to 780 nm (visible light spectrum) [2]. Commercially, there is an enormous interest of multinational companies specialized in light-emitting devices of finding new luminescent materials with adjustable visible light emissions for the improvement of lasers, light-emitting diodes, lamps, displays and so on.

In recent years, photoluminescence (PL) emissions of different silver-based semiconductors have been widely studied for these technological purposes [3,4]. However, few studies have been focused on the physical and chemical properties of silver pyrophosphate ($\text{Ag}_4\text{P}_2\text{O}_7$). In our knowing, Takahashi et al. [5] were the first to investigate this oxide by analyzing its ionic conductivity properties. It was only from 1986, when Koizumi et al. [6] published their research on high-pressure polymorphs in $\text{Ag}_4\text{P}_2\text{O}_7$ single crystals, that the structural features of this material began to be explored [7,8].

In the present study, $\text{Ag}_4\text{P}_2\text{O}_7$ powders were synthesized via different approaches: chemical precipitation (CP), conventional hydrothermal (CH) and microwave-assisted hydrothermal (MH).

The influence of structural and morphological aspects on the PL response at room temperature was also explored.

2. Materials and methods

2.1. Synthesis

Potassium pyrophosphate ($\text{K}_4\text{P}_2\text{O}_7$, 99%, Aldrich), silver nitrate (AgNO_3 , 99.8%, Vetec) and ammonium hydroxide (NH_4OH , 30%, Synth) were chosen as chemical starting precursors. For the CP reaction, NH_4OH was dripped into 0.02 M AgNO_3 solution heated at 90 °C until a transparent solution formed. Thereafter, 0.025 M $\text{K}_4\text{P}_2\text{O}_7$ solution was added into the previously prepared mixture, which was maintained for 30 min under stirring. The obtained precipitates were centrifuged, washed with deionized water/acetone, and dried at 60 °C for 2 h. This experimental procedure was also adopted in CH and MH, except that after mixing both AgNO_3 and $\text{K}_4\text{P}_2\text{O}_7$ solutions, the resulting solution was immediately transferred into an autoclave (stainless – CH and Teflon – MH). The hydrothermal treatment was performed at 100, 120 and 140 °C for 1 h.

2.2. Characterization

X-ray diffraction (XRD) patterns were recorded on a XRD-6000 diffractometer (Shimadzu, Japan) with $\text{CuK}\alpha$ radiation ($\lambda = 0.154184$ nm) by using a scanning scan rate of 0.2°/min and step size of 0.02°. Raman spectra were registered on a Senterra

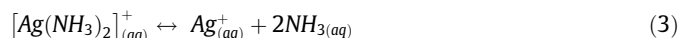
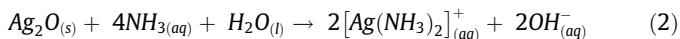
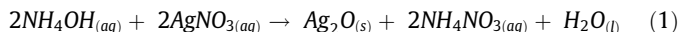
* Corresponding author.

E-mail address: jcsfisica@gmail.com (J.C. Sczancoski).

Raman scattering microscope (Bruker Optik, Germany) equipped with a laser of 532 nm and operated at 2 mW. The infrared (IR) spectrum was acquired on an Equinox 55 Fourier-transform infrared spectrometer (Bruker Optik, Germany). The morphological aspects were monitored on an Inspect F50 scanning electron microscopy (SEM) (Philips-FEI, Netherlands). Ultraviolet–visible (UV–vis) spectra were taken on a Cary 5G spectrophotometer (Varian, USA) operated in diffuse-reflection mode. PL spectra were analyzed at room temperature on a Fluorolog-3 FL3-122 spectrofluorometer (Horiba Jobin Yvon, Japan) equipped with a xenon lamp (450 W).

3. Results and discussion

Fig. 1(A–B) shows the XRD patterns of as-synthesized powders. In a first observation, $\text{Ag}_4\text{P}_2\text{O}_7$ formed by the CP reaction presented a typical diffractogram belongs to hexagonal phase, as reported in other published studies [6,7,9]. In this case, CP performed at 90 °C for 30 min provided a thermodynamically favorable condition for the gradual decomposition of silver diamine complex, $[\text{Ag}(\text{NH}_3)_2]^+$. The Ag^+ ions released in solution were bound to those of $\text{P}_2\text{O}_7^{4-}$, forming the $\text{Ag}_4\text{P}_2\text{O}_7$ phase (Eqs. (1)–(4) and Fig. S1 in Supplementary Data (SD)):



A curious behavior was detected for the powders conditioned to the CH environmental, which were influenced by the temperature processing. At 100 °C, a preferred crystallographic orientation phenomenon was identified because of strong XRD peaks found at 26.0° and 39.6°, corresponding to (0 0 1 2) and (0 0 1 8) planes, respectively. This behavior can be ascribed to slow transferring energy (thermal conduction and convection) imposed by the CH, whose reaction system takes much longer to achieve the target temperature. Therefore, the crystallites in the material had sufficient time to orient themselves in certain crystallographic planes. This preferred orientation was not observed at 120 °C. When the temperature was increased at 140 °C, a phase transition from $\text{Ag}_4\text{P}_2\text{O}_7$ to silver phosphate (Ag_3PO_4) was perceived (* in Fig. 1(A)). This Ag_3PO_4 phase was formed due to hydration of $\text{P}_2\text{O}_7^{4-}$ [7].

Adopting these same temperatures in MH, in which the microwaves were the energy source, XRD patterns showed peaks related to hexagonal phase. No signal of preferential orientation was observed; however, small traces of Ag_3PO_4 was evidenced for the powders hydrothermalized at 140 °C (* in Fig. 1(B)). These results denote that the microwave irradiation promoted a fast and homogeneous heating of the solution (dipolar polarization and ionic conduction), accelerating the decomposition of $[\text{Ag}(\text{NH}_3)_2]^+$ to release Ag^+ ions [10]. Although these events were very fast, the system was not able to stabilize only the $\text{Ag}_4\text{P}_2\text{O}_7$ phase at 140 °C.

Infrared spectroscopy was used as a tool to extract any structural information of $\text{Ag}_4\text{P}_2\text{O}_7$ as well as to probe the possible molecules adsorbed. In IR spectra (Fig. 1(C–D)), four absorption bands assigned to $\text{P}_2\text{O}_7^{4-}$ were distinguished at around 546 ($\delta_{\text{as}}\text{PO}_3$), 705 ($\nu_3\text{POP}$), 907 ($\nu_{\text{as}}\text{POP}$) and 1117 cm^{-1} ($\nu_3\text{PO}_3$) [11]. The bands from 2800 to 3350 cm^{-1} are arising from N–H and O–H bonds, as a consequence of ammonia and water molecules adsorbed on the powders. The other band of water adsorbed was seen at 1677 cm^{-1} . It is

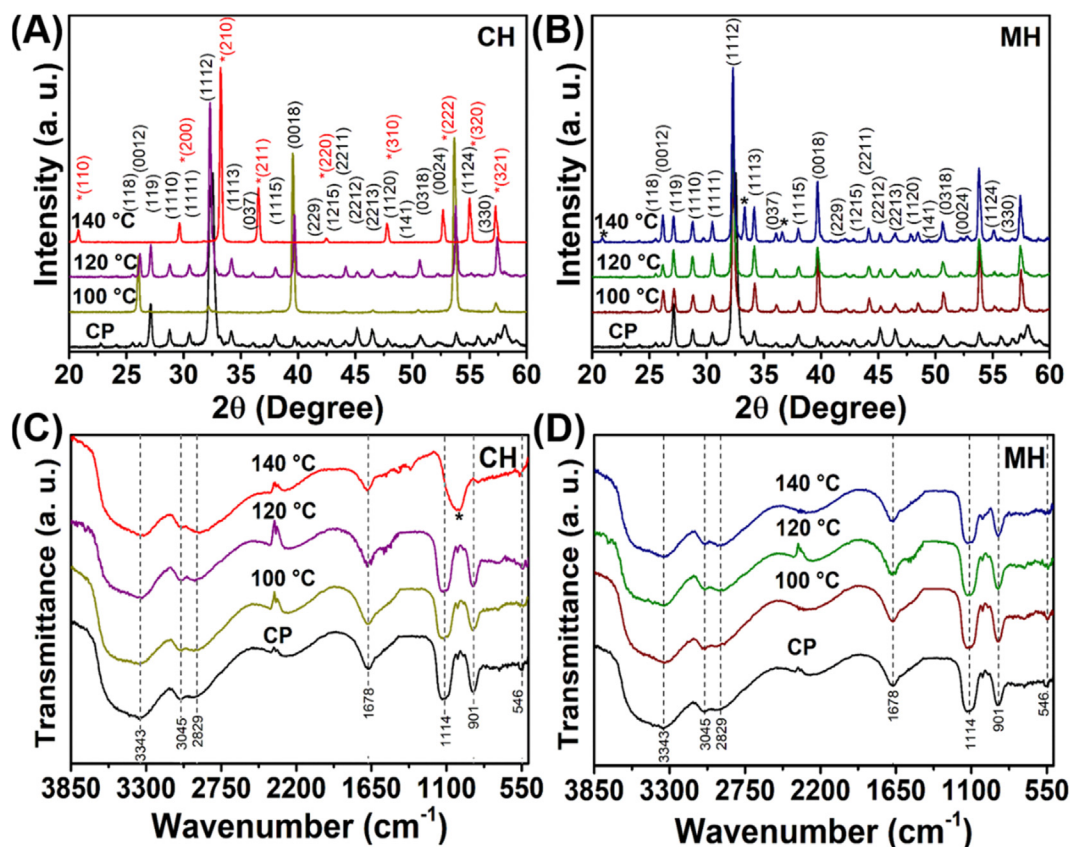


Fig. 1. (A–B) XRD patterns and (C–D) IR spectra of as-synthesized $\text{Ag}_4\text{P}_2\text{O}_7$ powders.

important to emphasize that the powders synthesized at 140 °C in CH presented a band at 1014 cm^{-1} provoked by PO_4^{3-} [10]. To corroborate with the structural data of as-synthesized powders, the Raman spectroscopy was also performed. All Raman spectra

revealed characteristic Raman-active bands related to vibrational frequencies of $\text{P}_2\text{O}_7^{4-}$ (Fig. S2 in SD).

Exploring the morphological behavior via SEM images, a system composed of doughnut/hexagonal-shaped microparticles was

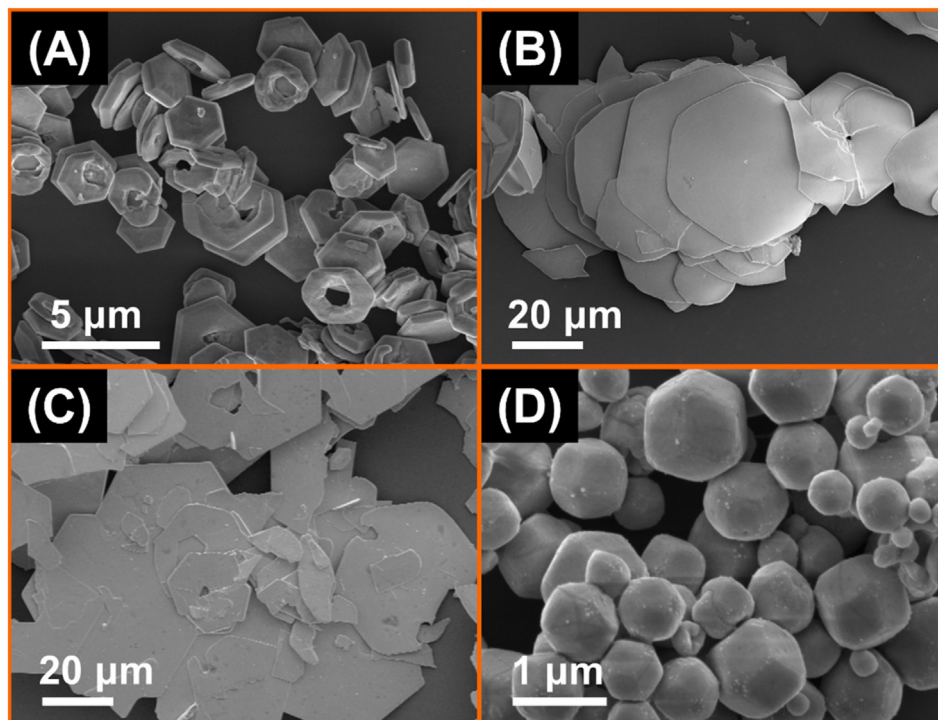


Fig. 2. SEM images of $\text{Ag}_4\text{P}_2\text{O}_7$ powders synthesized by (A) CP and CH at 100 °C (B), 120 °C (C) and 140 °C (D) for 1 h.

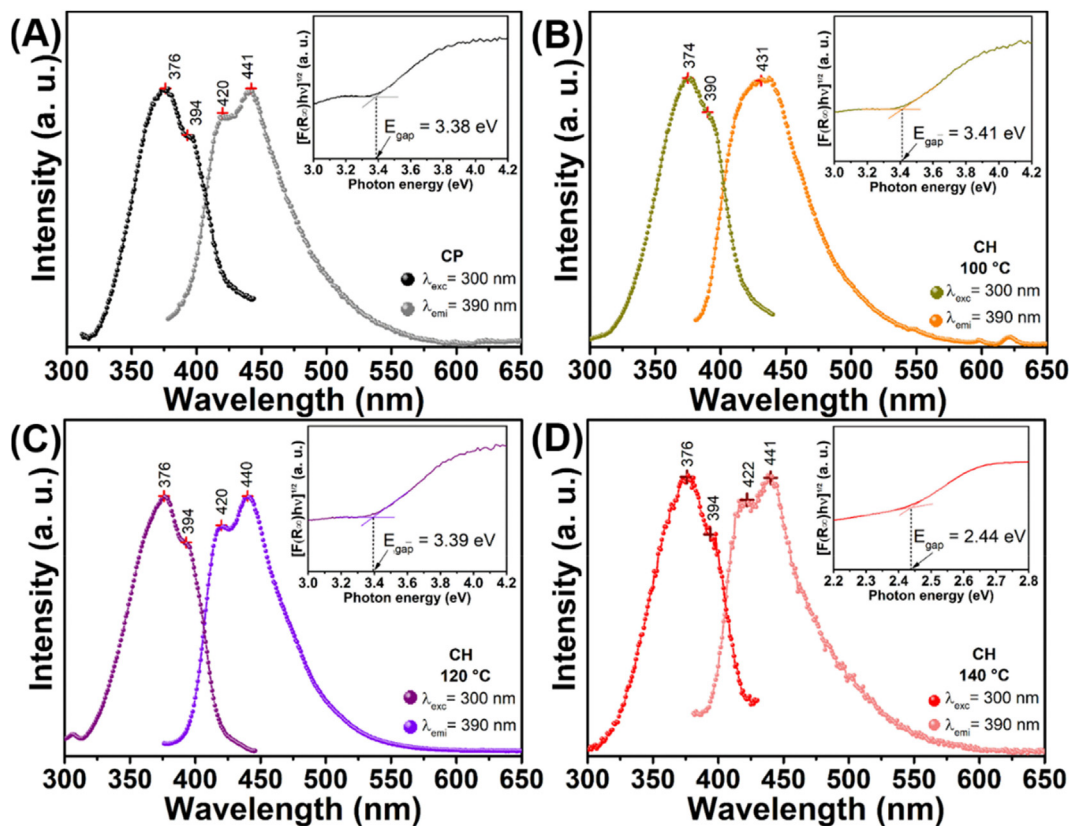


Fig. 3. Excitation and emission PL spectra of $\text{Ag}_4\text{P}_2\text{O}_7$ powders synthesized by (A) CP and (B-D) CH. Insets show the respective E_{gap} .

observed for $\text{Ag}_4\text{P}_2\text{O}_7$ synthesized by the CP. These particle shapes also presented surface defects (irregularities), Fig. 2(A). The temperature was the driving force to promote the break of $[\text{Ag}(\text{NH}_3)_2]^+$ and induce the supersaturation of the solution. Hence, the morphological control was affected in CP by a competitive effect between nucleation and growth. Due to the slow release of Ag^+ ions in a saturated medium of $\text{P}_2\text{O}_7^{4-}$, some nuclei were being formed while other particles were evolving to a grow stage. When submitted to CH at 100 and 120 °C, these microparticles grew, but they presented a morphological fragility (easily breakable), Fig. 2(B-C). These morphological changes can be arising from a dissolution-recrystallization process in a classical crystallization pathway [12]. As provided by XRD, the temperature of 140 °C favored only the growth of rhombic dodecahedron-shaped Ag_3PO_4 microparticles, Fig. 2(D) [10].

A similar behavior of these microparticles was noted in MH; however, several surface defects were verified in the microparticles submitted at 120 °C. In addition, at 140 °C was registered a mixture of hexagonal-shaped $\text{Ag}_4\text{P}_2\text{O}_7$ microparticles and rhombic dodecahedron-shaped Ag_3PO_4 microparticles in a same system (Fig. S3 in SD), in agreement with XRD patterns.

The optical band gap energy (E_{gap}) was estimated via UV-vis spectroscopy by employing the Kubelka-Munk method [13] for indirect transitions [14]. The E_{gap} values slightly oscillated from 3.36 to 3.41 eV, the only exception was the powder treated at 140 °C in CH (2.44 eV) because the single Ag_3PO_4 phase (Fig. 3 and Fig. S4 in SD).

In relation to excitation spectra was identified maximum points from 376 nm (3.3 eV) to 400 nm (3.1 eV). When compared to E_{gap} results, the electronic transitions were arising from intermediary energy levels in the band gap (deep- and shallow-level defect states) due to distortions on P-O bonds of $\text{P}_2\text{O}_7^{4-}$ [3,15]. This information can be confirmed by PL emission spectra, which exhibited a broadband profile. The maximum emissions were verified in violet/blue regions, indicating a superior contribution of shallow-level defect states (Fig. 3 and Fig. S4 in SD).

4. Conclusion

$\text{Ag}_4\text{P}_2\text{O}_7$ powders were successfully prepared via CP, CH and MH approaches. Single hexagonal $\text{Ag}_4\text{P}_2\text{O}_7$ phase was obtained by CP and hydrothermal treatments performed at 100 and 120 °C. The break of $[\text{Ag}(\text{NH}_3)_2]^+$ contributed to the appearance of doughnut/hexagonal-shaped microparticles. These microparticles grew and became easily broken in CH and MH. The maximum blue PL emissions were related to additional levels caused by shallow-level defect states.

Conflict of interest

None declared.

Acknowledgments

The authors are grateful to FAPESP (2015/11917-8; 2012/14004-5), CNPq and CAPES for the financial support.

Appendix A. Supplementary data

Supplementary data to this article can be found online at <https://doi.org/10.1016/j.matlet.2019.04.038>.

References

- [1] H.T. Lawless, H. Heymann, *Sensory evaluation of food: principles and practices*, Springer Science & Business Media, 2010.
- [2] G.A. Klein, T. Meyrath, *Industrial color physics*, Springer, 2010.
- [3] G. Botelho, J.C. Sczancoski, J. Andres, L. Gracia, E. Longo, Experimental and theoretical study on the structure, optical properties, and growth of metallic silver nanostructures in Ag_3PO_4 , *J. Phys. Chem. C* 119 (11) (2015) 6293–6306.
- [4] W.S. Pereira, M.M. Ferrer, G. Botelho, L. Gracia, I.C. Nogueira, I.M. Pinatti, I.L.V. Rosa, F.A. La Porta, J. Andres, E. Longo, Effects of chemical substitution on the structural and optical properties of $\alpha\text{-Ag}_{2-2x}\text{Ni}_x\text{WO}_4$ ($0 < x < 0.08$) solid solutions, *PCCP* 18 (31) (2016) 21966–21975.
- [5] T. Takahashi, S. Ikeda, O. Yamamoto, Solid-state ionics-solids with high ionic conductivity in the systems silver iodide-silver oxyacid salts, *J. Electrochem. Soc.* 119 (4) (1972) 477–482.
- [6] H. Koizumi, T. Hirono, T. Yamada, Y. Miyamoto, N. Ogawa, M. Koizumi, M. Shimada, High-pressure polymorph of silver pyrophosphate $\text{Ag}_4\text{P}_2\text{O}_7$, *Mater. Res. Bull.* 21 (7) (1986) 817–821.
- [7] L. Song, Y. Li, H. Tian, X. Wu, S. Fang, S. Zhang, Synthesis of $\text{AgBr}/\text{Ag}_4\text{P}_2\text{O}_7$ composite photocatalyst and enhanced photocatalytic performance, *Mater. Sci. Eng., B* 189 (2014) 70–75.
- [8] J. Zhao, Z. Ji, C. Xu, X. Shen, L. Ma, X. Liu, Hydrothermal syntheses of silver phosphate nanostructures and their photocatalytic performance for organic pollutant degradation, *Cryst. Res. Technol.* 49 (12) (2014) 975–981.
- [9] T. Yamada, H. Koizumi, Czochralski growth of $\text{Ag}_4\text{P}_2\text{O}_7$ crystals, *J. Cryst. Growth* 64 (3) (1983) 558–562.
- [10] G. Botelho, J. Andres, L. Gracia, L.S. Matos, E. Longo, Photoluminescence and photocatalytic properties of Ag_3PO_4 microcrystals: an experimental and theoretical investigation, *ChemPlusChem* 81 (2) (2016) 202–212.
- [11] S.A. Suthanthiraraj, R. Sarumathi, A new silver ion conducting $\text{SbI}_3\text{-Ag}_4\text{P}_2\text{O}_7$ nanocomposite solid electrolyte, *Appl. Nanosci.* 3 (6) (2012) 501–508.
- [12] F.C. Meldrum, H. Cölfen, Controlling mineral morphologies and structures in biological and synthetic systems, *Chem. Rev.* 108 (11) (2008) 4332–4432.
- [13] L. Tolvaj, K. Mitsui, D. Varga, Validity limits of Kubelka-Munk theory for DRIFT spectra of photodegraded solid wood, *Wood Sci. Technol.* 45 (1) (2010) 135–146.
- [14] T. Hirono, M. Fukuma, T. Yamada, Photoinduced effects in $\text{Ag}_4\text{P}_2\text{O}_7$ single crystals, *J. Appl. Phys.* 57 (6) (1985) 2267–2270.
- [15] S.K. Rout, L.S. Cavalcante, J.C. Sczancoski, T. Badapanda, S. Panigrahi, M. Siu Li, E. Longo, Photoluminescence property of powders prepared by solid state reaction and polymeric precursor method, *Physica B Condens. Matter.* 404 (20) (2009) 3341–3347.